DOI: https://doi.org/10.17816/onco633809

Intraoperative staining of malignant lung tumors using bioorganic fluorescent gold nanoclusters bound to aptamers

Galina S. Zamay[1, 2], Tatiana N. Zamay[1, 2], Daniil S. Chumakov[3], Semen A. Sidorov[1, 4], Aleksey V. Krat[1, 4], Boris N. Khlebtsov[3, 5], Irina A. Shchugoreva[1, 2], Anastasia A. Koshmanova[1], Ruslan A. Zukov[1, 4], Nikolai G. Khlebtsov[3, 5], Anna S. Kichkailo[1, 2]

[1] Professor V.F. Voino-Yasenetsky Krasnoyarsk State Medical University, Krasnoyarsk, Russia;
[2] Federal Research Center "Krasnoyarsk Science Center of the Siberian Branch of the Russian Academy of Sciences", Krasnoyarsk, Russia;
[3] Federal Research Centre "Saratov Scientific Centre of the Russian Academy of Sciences", Saratov, Russia;
[4] Krasnoyarsk Regional Clinical Oncology Dispensary named after A.I. Kryzhanovsky, Krasnoyarsk, Russia;
[5] Saratov State University, Saratov, Russia

ABSTRACT

BACKGROUND: The problem of recurrence, generalization, or metastasis of lung cancer remains relevant to this day, despite the advances in diagnostic and therapeutic methods of treatment. The main method of localized lung cancer treatment is surgery. The volume of resection is determined by the location of the tumor, its spread to surrounding tissues and the status of lymph node damage. However, even after removal of a large part of the lung, metastatic foci may remain in healthy tissue. To improve the effectiveness of diagnostics during surgery, fluorescence-navigated surgery can be used, based on the use of fluorescent dyes, which enables to see even small clusters of malignant cells in the early stages of tumor process development.

AIM: To develop a drug for fluorescence-navigation surgery based on aptamers and fluorescent gold nanoclusters (fluorescence excitation wavelengths are 365–410 nm, emission wavelengths are 615–650 nm).

MATERIALS AND METHODS: The object of the study is primary cultures of non-small cell lung cancer. Liposomes functionalized with DNA aptamer LC-17 were used to deliver gold nanoclusters stabilized with glutathione (GSH-AuNC) or bovine serum albumin (BSA-AuNC) to lung cancer cells. Electron microscopic images of the synthesized nanoclusters were obtained using transmission electron microscopy. Analysis of the efficiency of tumor cell binding to aptamer-functionalized liposomes containing nanoclusters was performed using flow cytometry Lung adenocarcinoma tissue was used to evaluate the efficiency of fluorescent nanoclusters.

RESULTS: The diameter of BSA-AuNC and GSH-AuNC nanoclusters was 1.8±0.5 nm and 1.5±0.3 nm, respectively. When exciting by light with a wavelength of 365 nm, the maximum fluorescence emission for BSA-AuNCs was 655 nm, and for GSH-AuNCs — 613 nm. The fluorescence quantum yields for BSA-AuNCs and GSH-AuNCs were 6% and 14%, respectively. LC-17 aptamer-functionalized liposomes with included GSH-AuNC and BSA-AuNC effectively bound to lung adenocarcinoma cells and stained them.

CONCLUSION: The possibilityl of using gold nanoclusters stabilized by GSH-AuNC and BSA-AuNC for fluorescence-guided surgery is demonstrated.

Keywords: aptamer; fluorescent gold nanoclusters; liposomes; fluorescence-guided surgery; lung cancer.

To cite this article:
Zamay GS, Zamay TN, Chumakov DS, Sidorov SA, Krat AV, Khlebtsov BN, Shchugoreva IA, Koshmanova AA, Zukov RA, Khlebtsov NG, Kichkailo AS. Intraoperative staining of malignant lung tumors using bioorganic fluorescent gold nanoclusters bound to aptamers. *Russian Journal of Oncology.* 2024;29(2):82–92. DOI: https://doi.org/10.17816/onco633809

Submitted: 26.06.2024 **Accepted:** 28.10.2024 **Published online:** 09.11.2024

DOI: https://doi.org/10.17816/onco633809

Интраоперационное окрашивание злокачественных опухолей лёгкого с помощью биоорганических флуоресцентных золотых нанокластеров, связанных с аптамерами

Г.С. Замай[1, 2], Т.Н. Замай[1, 2], Д.С. Чумаков[3], С.А. Сидоров[1, 4], А.В. Крат[1, 4], Б.Н. Хлебцов[3, 5], И.А. Щугорева[1, 2], А.А. Кошманова[1], Р.А. Зуков[1, 4], Н.Г. Хлебцов[3, 5], А.С. Кичкайло[1, 2]

[1] Красноярский государственный медицинский университет имени В.Ф. Войно-Ясенецкого, Красноярск, Россия;
[2] Федеральный исследовательский центр «Красноярский научный центр Сибирского отделения Российской академии наук», Красноярск, Россия;
[3] Федеральный исследовательский центр «Саратовский научный центр Российской академии наук», Саратов, Россия;
[4] Красноярский краевой клинический онкологический диспансер имени А.И. Крыжановского, Красноярск, Россия;
[5] Саратовский национальный исследовательский государственный университет имени Н.Г. Чернышевского, Саратов, Россия

АННОТАЦИЯ

Обоснование. Проблема рецидивирования, генерализации или метастазирования рака лёгкого до настоящего времени остаётся актуальной, несмотря на развитие диагностических и терапевтических методов лечения. Основной метод лечения локализованного рака лёгкого — хирургический. Объём резекции определяется локализацией опухоли, её распространением на окружающие ткани и статусом поражения лимфоузлов. Однако даже после удаления большой части лёгкого в здоровой ткани могут оставаться метастатические очаги. Для улучшения эффективности диагностики при операции может применяться флуоресцентно-навигационная хирургия, основанная на использовании флуоресцентных красителей, позволяющая видеть даже небольшие скопления злокачественных клеток на ранних стадиях развития опухолевого процесса.

Цель. Разработка препарата для флуоресцентно-навигационной хирургии на основе аптамеров и флуоресцентных нанокластеров золота (длины волн возбуждения флуоресценции — 365–410 нм, длины волн эмиссии — 615–650 нм).

Материалы и методы. Объект исследования — первичные культуры немелкоклеточного рака лёгкого. Для доставки золотых нанокластеров, стабилизированных глутатионом (GSH-AuNC) или альбумином бычьей сыворотки (BSA-AuNC), к клеткам рака лёгкого использовали липосомы, функционализированные ДНК-аптамером LC-17. Электронно-микроскопические изображения синтезированных нанокластеров получали с помощью просвечивающей электронной микроскопии. Анализ эффективности связывания опухолевых клеток с функционализированными аптамерами липосомами, содержащими нанокластеры, проводили методом проточной цитометрии. Для оценки эффективности флуоресцентных нанокластеров использовали ткань аденокарциномы лёгкого.

Результаты. Диаметр нанокластеров BSA-AuNC и GSH-AuNC составил 1,8±0,5 и 1.5±0.3 нм, соответственно. При возбуждении светом с длиной волны 365 нм максимум эмиссии флуоресценции для BSA-AuNC составил 655 нм, а для GSH-AuNCs — 613 нм. Квантовые выходы флуоресценции для BSA-AuNC и GSH-AuNC составили 6 и 14%, соответственно. Функционализированные аптамером LC-17 липосомы с включёнными в них GSH-AuNC и BSA-AuNC эффективно связывались с клетками аденокарциномы лёгкого и окрашивали их.

Заключение. Показана потенциальная возможность использования золотых нанокластеров, стабилизированных GSH-AuNC и BSA-AuNC, для флуоресцентно-навигационной хирургии.

Ключевые слова: аптамер; флуоресцентные золотые нанокластеры; липосомы; флуоресцентно-навигационная хирургия; рак лёгкого.

Как цитировать:
Замай Г.С., Замай Т.Н., Чумаков Д.С., Сидоров С.А., Крат А.В., Хлебцов Б.Н., Щугорева И.А., Кошманова А.А., Зуков Р.А., Хлебцов Н.Г., Кичкайло А.С. Интраоперационное окрашивание злокачественных опухолей лёгкого с помощью биоорганических флуоресцентных золотых нанокластеров, связанных с аптамерами // Российский онкологический журнал. 2024. Т. 29, № 2, С. 82–92. DOI: https://doi.org/10.17816/onco633809

Рукопись получена: 26.06.2024 **Рукопись одобрена:** 28.10.2024 **Опубликована online:** 09.11.2024

BACKGROUND

Currently, despite the development of the diagnostic and therapeutic methods of the lung cancer treatment methods, the problem of its recurrence, generalization, or metastatic spread remains relevant. The non-small cell lung cancer (NSCLC) recurrence rate in the late postoperative period is about 45% [1], and its localization varies depending on the disease stage. Thus, 73% of cases can show distant metastases, 19% can show locoregional ones, and 7% can show both types of metastases combined [2].

The primary treatment method for the localized lung cancer is surgery. The extent of resection is determined by the tumor localization, its spread into the adjacent tissues, and the lymph nodes' lesion status. In cases of malignant lesions of the lobar or primary bronchi, bronchoplastic surgery is possible [3]. Nevertheless, even after resection of a large part of a lung, metastatic foci can remain in the healthy tissue because of their insufficient size and degree of malignancy to be visually different from it.

The malignant cells continue their mitosis after therapy, which leads to locoregional recurrencies and metastatic spread into distant organs. To improve the intraoperative diagnosing, the fluorescent dye-based fluorescence-guided surgery (FGS) can be used. This procedure allows surgeons to see small clusters of malignant cells at the low tumor stages.

To this date, many FGS studies using different molecular complexes of fluorescent dyes with specific ligands, such as antibodies, peptides, or aptamers, have been performed. Some products are already undergoing clinical or preclinical trials [4].

The infrared dyes have become especially popular in FGS due to their low background fluorescence and deep penetration of radiation. The limitations inherent to such dyes include the necessity of specialized equipment; besides, when using the infrared FGS mode, surgeons can visualize only the fluorescence of the dye, which makes the topography of tissues eye-imperceptible. The antibodies or peptides used in the available targeted dyes for fluorescence-guided diagnostics are immunogenic and can cause severe allergic reactions in patients [5].

Consequently, the development of the new targeted fluorescent complexes with the surgery-optimal optical characteristics — high specificity, high tumor fluorescence to background ratio, and low toxicity — is relevant.

In this study we present the liposome- and aptamer-based conjugates delivering in a targeted way the gold nanoclusters into tumor that can excite and emit in the range of porphyrin-IX (excitation: 400–410 nm, emission: 650–710 nm). Such dyes can be visualized using surgical fluorescent microscopes or by naked eye under ultraviolet excitation. A substantial advantage of the dyes emitting in this range is the absence of the tissues' autofluorescence, which ensures a better contrast of the stained tumor areas.

The aptamers are the preferrable targeting agents due to their low immunogenicity, small sizes (favoring their penetration into tissues and rapid clearance), availability, and simple chemical synthesis and modifications [6].

The fluorescent gold nanoclusters (AuNCs) are ultra-small (1–3 nm) complexes of organic ligands-stabilized gold atoms. AuNCs have the properties that make them promising agents for the intraoperative fluorescent diagnostics. The advantages of AuNCs are the relatively simple synthesis, high photostability, the possibility of the fluorescence emission spectral tuning, and a large Stokes shift. AuNCs are less toxic than inorganic quantum dots. The best studied and characterized nanoclusters are the gold nanoclusters stabilized with glutathione (GSH-AuNCs) and bovine serum albumin (BSA-AuNCs), which have higher quantum efficiencies of fluorescence compared with other nanostructures of this type [7, 8].

Aim. To develop a product for FGS based on aptamers and fluorescent gold nanoclusters (fluorescence excitation wavelengths: 365–410 nm, emission wavelengths: 615–650 nm).

MATERIALS AND METHODS

Study design

The flow cytometry used primary cultures of lung adenocarcinoma. To visually evaluate the binding of complexes, postoperative tissues of lung adenocarcinoma were used.

The study included the samples from 4 patients with NSCLC. The detailed description is presented in Table 1, all the diagnoses are morphology-confirmed.

Study duration and setting

The gold nanoclusters were received and defined in the Institute of Biochemistry and Physiology of Plants and Microorganisms (IBPPM) of the Federal Research Center Saratov Scientific Center of the Russian Academy of Sciences. The studies were carried out from March 2021 to December 2023. The complexes of nanoclusters in aptamer-modified liposomes were received on the basis of the Laboratory of Numerical Controlled Medicines and Theranostics of the Federal Research Center Krasnoyarsk Science Center of the Siberian Branch of the Russian Academy of Sciences January to March 2024. The analysis of the complexes binding to the primary cultures and postoperative materials was performed from March 2024 to May 2024 on the basis of the Laboratory of Biomolecular and Medical Technologies of the Krasnoyarsk State Medical University named after Professor V. F. Voyno-Yasenetsky under the Ministry of Health of the Russian Federation.

DOI: https://doi.org/10.17816/onco633809

Table 1. Postoperative tissue samples included in the study

Test	Sample type	Histological type	Stage
Flow cytometry	Primary culture	Adenocarcinoma	T4N3M0
		Adenocarcinoma	T3N2M0
		Adenocarcinoma	T4N2M0
Visual assessment	Postoperative tissue	Adenocarcinoma	T3N0M0

Study object

The tumor tissues were obtained from NSCLC patients, who received radical surgeries in the A. I. Kryzhanovsky Krasnoyarsk Regional Clinical Oncology Dispensary. Before sampling, written informed consents to analyze the postoperative materials in the Research and Development Laboratory were obtained from all the patients. The tumor tissues were aseptically resected and placed into cooled DMEM with penicillin and streptomycin. The samples were delivered to the laboratory within two hours after resection for the further investigation and cultivation of cells.

The study used the LC-17 DNA-aptamer to the NSCLC tumor cells [9]. The aptamer's specificity to the tissue cells, circulating tumors, and plasma proteins was pre-studied [10, 11].

Cell isolation and cultivation

The tumor tissues were washed in the DMEM. The tissues were minced, the vessels, necrotic foci, and thrombi were removed. The resulting tissues were dissociated using a dosage device. Then the suspension was filtered through a 70-μm filter and sedimented twice by centrifuging at 2000 rpm for 5 minutes. The sediment was resuspended in 2 mL of DPBS, then covered with 3 mL of lymphocytes separation media, and centrifuged for 10 minutes at 2000 rpm. The cell layer at the lymphocytes separation media/DPBS interface was collected and transferred into a sterile tube with DPBS, and then centrifuged for 5 minutes at 2000 rpm. The sediment was transferred into a cultivation tube or container with the medium (DMEM, 10% of plasma fetal calf serum, 20 μg/mL of insulin, 10 μg/mL of transferrin, 25 nmol/L of sodium selenite, 100 U/mL of antibiotics, and 1 ng/mL of epidermal growth factor) and cultivated in an atmosphere with 5% CO_2 at 37°C. When the cells reached confluence, they were dispersed with the Trypsin-Versene regenerant solution for subcultivation of cells. The cells were washed in a Ca^{2+} and Mg^{2+}-containing phosphate buffer by centrifuging for 3 minutes at 2500 rpm and cultivated in the cultivation medium containing DMEM, 5% of plasma fetal calf serum, 20 μg/mL of insulin, 10 μg/mL of transferrin, 25 nmol/L of sodium selenite, and 100 U/mL of antibiotics.

Preparation of liposomes

To prepare the liposomes, a lipid mixture containing cholesterol, L-α-phosphatidylcholine, and stearylamine (kit for liposomes, Sigma-Aldrich, Germany) was used. The L-α-phosphatidylcholine/stearylamine/cholesterol molar ratio in the mixture was 63:18:9, respectively. The liposomes were prepared using the thin film hydration method with subsequent sonication. The lipids were initially dissolved in 5 mL of chloroform/methanol mixture (3:1). The solvent was evaporated in a rotary evaporator to obtain a dry film of lipids. Then the dry film of lipids was hydrated by adding 50 mL of DPBS (pH 7.4) at ambient temperature for 10 minutes. Following the hydration, the liposomes were ultrasonicated for 30 minutes at 25°C to ensure the correct mixing and formation of liposomes. The resulting liposomes were stored at 4°C for subsequent use.

Functionalization of liposomes

The liposomes were functionalized with the LC-17 aptamer, modified with cholesterol at the 3'-end, and methyl fluorescein f (FAM) at the 5'-end, at a final concentration of 0.5 μM. To incorporate the aptamer into the lipid layer of liposomes, the sample was incubated at 60°C for one hour. Once incubated, the mixture was immediately placed on ice for 5 minutes to restore the aptamer's conformation.

Synthesis and characterization of fluorescent gold nanoclusters

All the synthesis glassware was pre-washed with aqua regia (HCl/HNO_3=3:1), and then rinsed with ethanol and water. To synthesize the glutathione-based fluorescent AuNCs (GSH-AuNC), the following technique was used. 1.5 mL of 100 mM of reduced glutathione solution and 43.5 mL of H_2O were mixed in a glass vial and stirred. Then the resulting solution was spiked with 5 mL of 20 mM $HAuCl_4$. The resulting mixture was stirred for 2 minutes. After that the reaction mixture was incubated in a thermostat for 24 hours at 70°C without stirring. To synthesize the albumin-stabilized fluorescent gold nanoclusters (BSA-AuNCs), the following technique was used. 25 mL of 38.4-mg/mL BSA and 25 mL of 11.6-mM $HAuCl_4$ were mixed in a glass vial. The mixture was intensively stirred in a magnetic stirrer for 2 minutes. At the next stage, the reaction mixture was spiked with 2 mL of 1 M NaOH. Then the reaction mixture was heated at 90 °C for 45 minutes with intensive stirring.

The electron microscopy images of the synthesized nanoclusters were obtained using the transmission electron microscopy. The microscopic images were obtained using the Libra-120 (Carl Zeiss, Germany) microscope in the Simbioz Center for Collective Use of Research Equipment in Physicochemical Biology and Nanobiotechnology of the Institute of Biochemistry and Physiology of Plants and Microorganisms, Russian Academy of Sciences (IBPPM RAS). The fluorescence excitation and emission spectra of the synthesized nanodyes were recorded using the Cary Eclipse (Agilent, USA) spectrofluorometer.

Introduction of nanodyes (GSH-AuNC and BSA-AuNC) into LC-17 aptamer-functionalized liposomes

The liposomes were incubated with nanoclusters in a shaker at 4°C for 12 hours. This allowed the fluorophores to enter into liposomes. After loading nanoclusters, the liposomes were transferred into a dialysis sac and put into a Ca^{2+}- and Mg^{2+}-containing phosphate buffer for 5 hours at 4°C to remove the excessive fluorophores that did not enter into liposomes. To destroy the existing aggregates and ensure the uniform distribution of liposomes, the suspension was placed in an ultrasonic bath for 30 minutes.

Analysis of efficiency of binding of tumor cells with nanoclusters-containing and aptamer-functionalized liposomes

The binding of the gold nanoclusters-containing liposomes with the lung cancer cells was analyzed using the FC-500 (Beckman Coulter Inc., USA) flow cytometer. The culture-derived lung cancer cells were pre-incubated with 1 ng/μL of yeast RNA for 30 minutes in a shaker at ambient temperature.

Then the cell mixture was incubated for 30 minutes at ambient temperature with the GSH-AuNC- and BSA-AuNC-containing liposomes bound to LC-17 aptamer. To avoid the non-specific binding of the lung cancer cells with liposomes, the mixture was washed by centrifuging at 3000 rpm for 5 minutes. The findings were analyzed using the Kaluza® 1.1 (Beckman Coulter Inc., USA) software.

Postoperative tissue staining

To evaluate the efficiency of the fluorescent nanocomplexes, the T3N0M0 adenocarcinomal tissue of the right lung middle lobe was used. The diagnosis was morphology-confirmed. The nanocomplexes were applied onto the lung tissue; to visualize the binding, an ultraviolet radiation source was used. Upon 3 minutes after staining, the tissue was three times washed with phosphate buffer; and the luminescence was evaluated.

Ethical review

The study was approved by the Ethics Committee of the Krasnoyarsk State Medical University (Confirmation No. 37/2012 of 01/31/2012).

Statistical analysis

The morphometric parameters of nanoclusters were obtained by calculating the ensemble of 200 nanoclusters in the electron microscopy images. The findings were presented as the arithmetic mean and its standard deviation (M±SD).

The findings were statistically processed using the Statistica 7.0 Software. The hypothesis of the statistical significance of differences between samples was checked using the Mann–Whitney test.

RESULTS

Characteristic of synthesized nanodyes

Various methods are used to obtain gold nanostructures, including the traditional chemical techniques of condensation and the environment-friendly "green" approaches, when gold is regenerated using plant extracts [12, 13]. The AuNC synthesis involved using organic ligands (L-glutathione and bovine serum albumin), which acted simultaneously as regenerating and stabilizing agents. Figure 1, *a*, *b* shows the transmission electron microscopy images and the fluorescence spectra of the synthesized nanoclusters. The estimate of the sizes of at least 100 particles in the transmission electron microscopy images found that the respective BSA-AuNC and GSH-AuNC diameters were 1.8±0.5 and 1.5±0.3 nm. At the excitation with a 365-nm wavelength light, the maximal emissions of fluorescence were 655 nm for BSA-AuNC and 613 nm for GSH-AuNC. The calculated quantum efficiencies of fluorescence for BSA-AuNC and GSH-AuNC were 6 and 14% respectively.

Creation of liposomes with aptamer-based incapsulated dyes

In this study, the BSA-AuNC and GSH-AuNC gold nanoclusters were incapsulated into liposomes with LC-17 aptamer. This allowed ensuring the delivery of the nanoparticles to the lung cancer cells. This technique has several advantages compared with the direct binding of aptamers to nanoclusters via functional groups. First, this enhances the intensity of fluorescence, as each liposome can carry several fluorophore molecules. Second, the toxicity reduces, as the dyes are not in direct contact with the patients' blood or tissues. Third, the complexes' circulation time elongates, their stability improves, and their targeted delivery is ensured.

DOI: https://doi.org/10.17816/onco633809

To visualize the aptamer-to-liposomes binding, the tertiary structure of the LC-17 aptamer was constructed (Figure 2, *a*). The complete aptamer–liposome–gold nanocluster complex is shown in Figure 2, *b*.

Evaluation of efficiency of binding of nanodyes incapsulated in aptamer-functionalized liposomes with tumor cells and tissues *ex vivo*

The efficiency of the binding of the nanodyes incapsulated in aptamer-functionalized liposomes was evaluated by flow cytometry using FC-500 (Beckman Coulter, USA) cytometer. The BSA-AuNC and GSH-AuNC nanoclusters demonstrated fluorescence in the red spectral range, while the FAM-labeled aptamer showed it in the green spectral range. Hence, the fluorescent signal was detected in two channels: FL1 for FAM, and FL4 for BSA-AuNC and GSH-AuNC.

To evaluate the efficiency of the nanoclusters' binding with biological samples, the primary lung cancer cultures from postoperative material were obtained.

Figure 3 shows that the fluorescent signals from the lung cancer culture cells themselves were not detected; however, when stained with the complexes that contained the LC-17 aptamer and the GSH-AuNC and BSA-AuNC nanodyes, they showed fluorescence in the FL1 and FL4 channels.

To evaluate the binding of the resulting nanostructure with the lung cancer tissue, the *ex vivo* tumor was divided into several parts and stained with one of the liposomes/nanodyes complexes or phosphate buffer for control (Figure 4).

Figure 4 shows that no autofluorescence of tumor was observed. The GSH-AuNC-containing LC-17 aptamer-functionalized liposomes were bound to the tumor tissue; this was confirmed by the visually red luminescence under ultraviolet light. The BSA-AuNC-containing

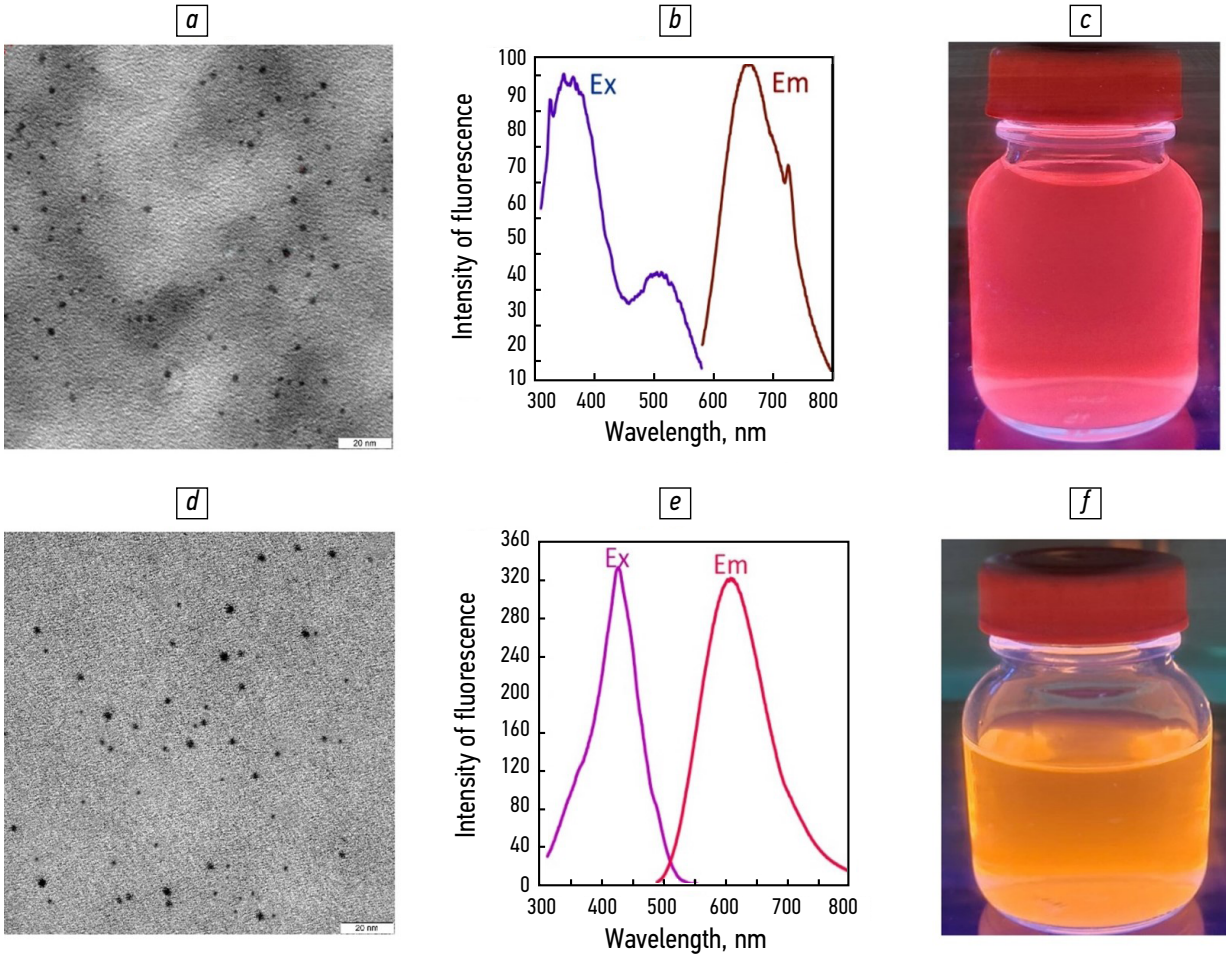

Fig. 1. The transmission electron microscopy images and the fluorescence spectra of the synthesized nanoclusters. *a* — transmission electron microscopy image of the BSA-AuNCs (scale bar is 20 nm); *b* — fluorescence spectra of the BSA-AuNCs; *c* — BSA-AuNCs suspension under ultraviolet lamp irradiation (365 nm); *d* — transmission electron microscopy image of the GSH-AuNCs (scale bar is 20 nm); *e* — fluorescence spectra of the GSH-AuNCs; *f* — GSH-AuNCs suspension under ultraviolet lamp irradiation (365 nm).

LC-17 aptamer-functionalized liposomes stained the tumor tissue as well.

DISCUSSION

FGS has not, yet, become wide-spread when resecting the main and metastatic tumor foci. Nevertheless, there are studies that confirm the promising outlook of this method, such as using the methylene blue, indocyanine green, or molecule specific to the lung adenocarcinoma folate receptor alpha [15, 16].

Thus, for example, C.H. Li et al. used the AS1411 aptamer-functionalized GSH-AuNC with diatrizoic acid (AS1411-DA-AuNC) to stain tumors in animal models [17]. In the above study, the aptamer was directly conjugated with AuNC using 1-ethyl-3-(3-dimethylaminopropyl)carbodiimide (EDC). However, this approach to conjugation has its limitations due to

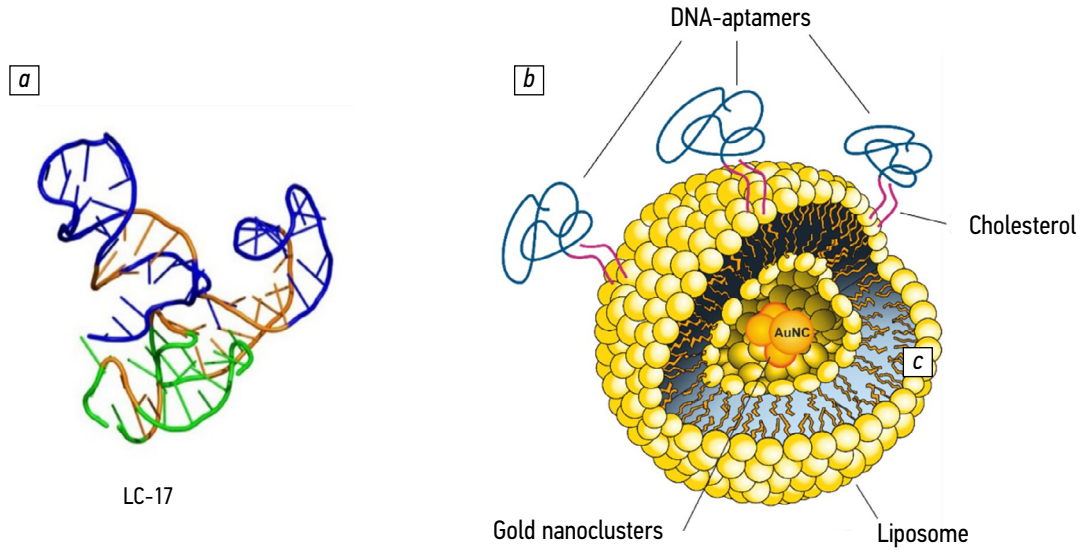

Fig. 2. The tertiary structure of the aptamer. *a* — the LC-17 aptamer model; *b* — a diagram depicting the LC17-liposome–gold nanoclaster.

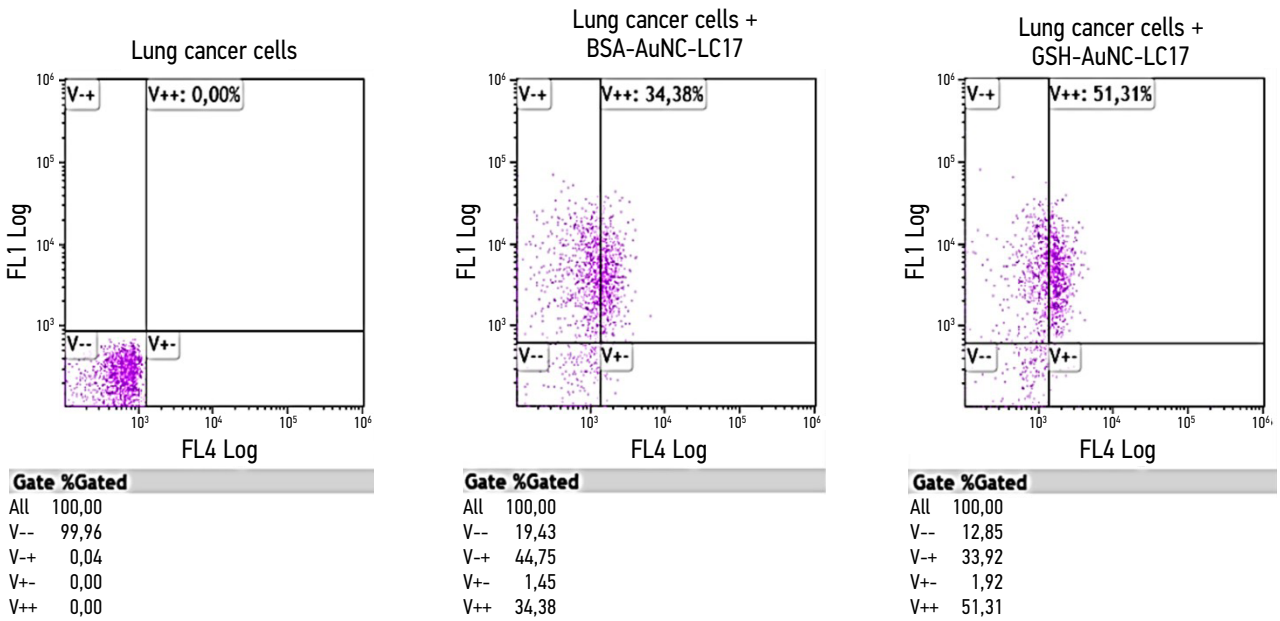

Fig. 3. Flow cytometry of lung cancer cells stained with liposomes containing GSH-AuNCs or BSA-AuNCs associated with the LC-17 aptamer.

the rapid hydrolysis of EDC in aqueous medium and to the fact that many gold nanoclusters are subject to biodegradation and aggregation in biologic medium.

The novelty of the approach proposed in this study consists in the original design of the complex consolidating the following three components:

- lung cancer cells-specific aptamer
- liposomes
- albumin- or glutathione-based fluorescent nanoclusters characterized by large Stokes shifts and relatively high quantum efficiencies of fluorescence.

From an oncology and health economics perspective, using the fluorescent methods of tumor visualization — at the diagnostic stage and during the radical resection of tumor — will allow avoiding the early recurrences of disease and repeated surgeries, reducing the number of the adjuvant antitumor therapy courses by increasing the radicality of the surgical treatment. Such approach to treatment will result in substantial savings on the healthcare costs and better quality of patients' lives. Noteworthy is that the greater diversity of the fluorescence inducers will extend the FGS range to other malignant neoplasms surgery areas and achieve more beneficial surgery outcomes for patients.

CONCLUSION

One of the most vital problems of surgery in lung cancer patients is visualization of not only the tumoral foci but also of the micrometastases as the malignant cells remaining in tissue continue proliferating, inducing recurrencies and disease progression. This study has investigated the possibility to use the BSA-AuNC and GSH-AuNC dyes-loaded and LC-17 aptamer-modified liposomes to identify tumoral foci during surgery. The possibility to visualize the tumor tissue during surgery was simulated with the postoperative material of a patient with lung adenocarcinoma using an ultraviolet radiation source. The potential possibility to integrate the BSA-AuNC and GSH-AuNC nanoclusters at the preoperative diagnostic stage to identify the metastatic foci with FGS was shown. Overall, the approach being developed has the potential to alter the treatment strategy for patients with NSCLC, considering both the criteria for radical surgery and alternative non-invasive treatment methods such as antitumoral and radiation therapies.

ADDITIONAL INFORMATION

Funding source. Research and publication were supported by the Ministry of Science and Higher Education of the Russian Federation FWES-2022-0005 (A.S.K.). The production and characterization of gold nanoclusters was carried out within the framework of the state assignment of the Ministry of Education and Science of the Russian Federation for the Federal Research Center "Saratov Scientific Center of the Russian Academy of Sciences", topic No. 1022040700960-1.

Competing interests. The authors declare that they have no competing interests.

Authors' contribution. All authors made a substantial contribution to the conception of the work, acquisition, analysis, interpretation of data for the work, drafting and revising the work, final approval of the version to be published and agree to be accountable for all aspects of the work. Zamay GS, Zamay TN — conducting research, analyzing and interpreting data, writing the text and editing the article; Chumakov DS — conducting research, analyzing and interpreting data, editing the manuscript; Sidorov SA, Khlebtsov BN — conducting research, analyzing and interpreting data; Krat AV, Shchugoreva IA — conducting research, analyzing data; Koshmanova AA — conducting research; Zukov RA — manuscript editing; Khlebtsov NG — concept of the work; Kichkaylo AS — research, data analysis, article editing.

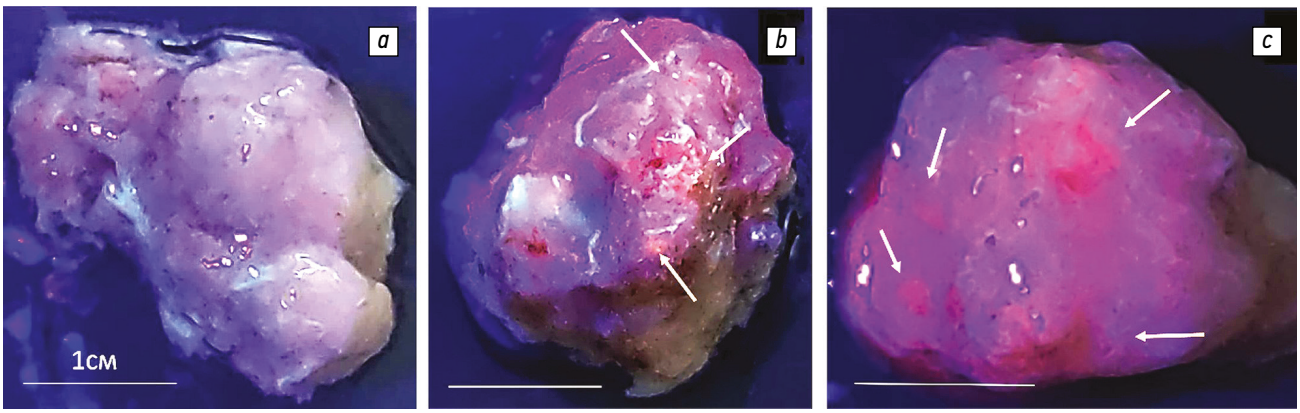

Fig. 4. *Ex vivo* staining of lung cancer tissue: *a* — without staining; *b* — stained with GSH-AuNCs in liposomes containing LC-17 aptamer; *c* — stained with BSA-AuNCs in liposomes containing LC-17 aptamer.

REFERENCES

1. Higgins KA, Chino JP, Berry M, et al. Local failure in resected stage N1 lung cancer: implications for adjuvant therapy. *International journal of radiation oncology, biology, physics.* 2012;83(2):727–733. doi: 10.1016/j.ijrobp.2011.07.018

2. Varlotto JM, Yao AN, DeCamp MM, et al. Nodal stage of surgically resected non-small cell lung cancer and its effect on recurrence patterns and overall survival. *International journal of radiation oncology, biology, physics.* 2015;91(4):765–773. doi: 10.1016/j.ijrobp.2014.12.028

3. Burel J, Ayoubi ME, Basté JM, et al. Surgery for lung cancer: postoperative changes and complications—what the Radiologist needs to know. *Insights into Imaging.* 2021;12:116. doi: 10.1186/s13244-021-01047-w

4. Jiao J, Zhang J, Yang F, et al. Quicker, deeper and stronger imaging: A review of tumor-targeted, near-infrared fluorescent dyes for fluorescence guided surgery in the preclinical and clinical stages. *European Journal of Pharmaceutics and Biopharmaceutics.* 2020;152:123–143. doi: 10.1016/j.ejpb.2020.05.002

5. Van Keulen S, Hom M, White H, Rosenthal EL, Baik FM. Evolution of fluorescence-guided surgery. *Molecular Imaging and Biology.* 2023;25:36–45. doi: 10.1007/s11307-022-01772-8

6. Krat AV, Zamay TN, Zamay GS, et al. The use of DNA aptamers in the estimation of the prevalence the tumor process in lung cancer patients. *Siberian Medical Review.* 2016;5(101):96–98. EDN: XDNMCL

7. Luo Z, Yuan X, Yu Y, et al. From aggregation-induced emission of Au(I)-thiolate complexes to ultrabright Au(0)@Au(I)-thiolate core-shell nanoclusters. *Journal of the American Chemical Society.* 2012;134(40):16662–16670. doi: 10.1021/ja306199p

8. Khlebtsov B, Tuchina E, Tuchin V, Khlebtsov N. Multifunctional Au nanoclusters for targeted bioimaging and enhanced photodynamic inactivation of Staphylococcus aureus. *RSC Advances.* 2015;5:61639–61649. doi: 10.1039/C5RA11713E

9. Zamay GS, Kolovskaya OS, Zamay TN, et al. Aptamers selected to postoperative lung adenocarcinoma detect circulating tumor cells in human blood. *Molecular Therapy.* 2015;23(9):1486–1496. doi: 10.1038/mt.2015.108

10. Zamay GS, Ivanchenko T, Zamay TN, et al. DNA-Aptamers for Characterization of Histological Structure of Lung Adenocarcinoma. *Molecular Therapy: Nucleic Acid.* 2016;17(6):150–162. doi: 10.1016/j.omtn.2016.12.004

11. Zamay GS, Zamay TN, Kolovskii VA, et al. Electrochemical aptasensor for lung cancer-related protein detection in crude blood plasma samples. *Scientific Reports.* 2016;6:34350. doi: 10.1038/srep34350

12. Chumakov D, Pylaev T, Avdeeva E, et al. Anticancer properties of gold nanoparticles biosynthesized by reducing of chloroaurate ions with Dunaliella salina aqueous extract. *Proc SPIE: Optical and Nano-Technologies for Biology and Medicine.* 2020;11457:e1145715. doi: 10.1117/12.2564630

13. Saleh SM, Almotiri MK, Ali R. Green synthesis of highly luminescent gold nanoclusters and their application in sensing Cu (II) and Hg (II). *Journal of Photochemistry and Photobiology A: Chemistry.* 2022;426:e113719. doi: 10.1016/j.jphotochem.2021.113719

14. Holt D, Okusanya O, Judy R, et al. Intraoperative near-infrared imaging can distinguish cancer from normal tissue but not inflammation. *PLoS One.* 2014;9(7):e103342. doi: 10.1371/journal.pone.0103342

15. Newton AD, Kennedy GT, Predina JD. Intraoperative molecular imaging to identify lung adenocarcinomas. *Journal of Thoracic Disease.* 2016;8(9S):S697–S704. doi: 10.21037/jtd.2016.09.50

16. Rynda AYu, Olyushin VE, Rostovtsev DM, Zabrodskaya YuM, Papayan GV. Comparative analysis of 5-ALA and chlorin E6 fluorescence-guided navigation in malignant glioma surgery. *Pirogov Russian Journal of Surgery*. 2022;(1):5–14. doi: 10.17116/hirurgia20220115

17. Li CH, Kuo TR, Su HJ, et al. Fluorescence-guided probes of aptamer-targeted gold nanoparticles with computed tomography imaging accesses for in vivo tumor resection. *Scientific Reports.* 2015;5:e15675. doi: 10.1038/srep15675

СПИСОК ЛИТЕРАТУРЫ

1. Higgins K.A., Chino J.P., Berry M., et al. Local failure in resected stage N1 lung cancer: implications for adjuvant therapy // International journal of radiation oncology, biology, physics. 2012. Vol. 83, N 2. P. 727–733. doi: 10.1016/j.ijrobp.2011.07.018

2. Varlotto J.M., Yao A.N., DeCamp M.M., et al. Nodal stage of surgically resected non-small cell lung cancer and its effect on recurrence patterns and overall survival // International journal of radiation oncology, biology, physics. 2015. Vol. 91, N 4. P. 765–773. doi: 10.1016/j.ijrobp.2014.12.028

3. Burel J., Ayoubi M.E., Basté J.M., et al. Surgery for lung cancer: postoperative changes and complications—what the Radiologist needs to know // Insights into Imaging. 2021. Vol. 12. P. 116. doi: 10.1186/s13244-021-01047-w

4. Jiao J., Zhang J., Yang F., et al. Quicker, deeper and stronger imaging: A review of tumor-targeted, near-infrared fluorescent dyes for fluorescence guided surgery in the preclinical and clinical stages // European Journal of Pharmaceutics and Biopharmaceutics. 2020. Vol. 152. P. 123–143. doi: 10.1016/j.ejpb.2020.05.002

5. Van Keulen S., Hom M., White H., Rosenthal E.L., Baik F.M. Evolution of fluorescence-guided surgery // Molecular Imaging and Biology. 2023. Vol. 25. P. 36–45. doi: 10.1007/s11307-022-01772-8

6. Крат А.В., Замай Т.Н., Замай Г.С., и др. Использование ДНК-аптамеров в оценке распространенности опухолевого процесса у больных раком легкого // Сибирское медицинское обозрение. 2016. Т. 5, № 101. С. 96–98. EDN: XDNMCL

7. Luo Z., Yuan X., Yu Y., et al. From aggregation-induced emission of Au(I)-thiolate complexes to ultrabright Au(0)@Au(I)-thiolate core-shell nanoclusters // Journal of the American Chemical Society. 2012. Vol. 134, N 40. P. 16662–16670. doi: 10.1021/ja306199p

8. Khlebtsov B., Tuchina E., Tuchin V., Khlebtsov N. Multifunctional Au nanoclusters for targeted bioimaging and enhanced photodynamic inactivation of Staphylococcus aureus // RSC Advances. 2015. Vol. 5. P. 61639–61649. doi: 10.1039/C5RA11713E

9. Zamay G.S., Kolovskaya O.S., Zamay T.N., et al. Aptamers selected to postoperative lung adenocarcinoma detect circulating tumor cells in human blood // Molecular Therapy. 2015. Vol. 23, N 9. P. 1486–1496. doi: 10.1038/mt.2015.108

10. Zamay G.S., Ivanchenko T., Zamay T.N., et al. DNA-Aptamers for Characterization of Histological Structure of Lung Adenocarcinoma // Molecular Therapy: Nucleic Acid. 2016. Vol. 17, N 6. P. 150–162. doi: 10.1016/j.omtn.2016.12.004

11. Zamay G.S., Zamay T.N., Kolovskii V.A., et al. Electrochemical aptasensor for lung cancer-related protein detection in crude blood plasma samples // Scientific Reports. 2016. Vol. 6. P. 34350. doi: 10.1038/srep34350

12. Chumakov D., Pylaev T., Avdeeva E., et al. Anticancer properties of gold nanoparticles biosynthesized by reducing of chloroaurate ions with Dunaliella salina aqueous extract // Proc SPIE: Optical and Nano-Technologies for Biology and Medicine. 2020. Vol. 11457. P. e1145715. doi: 10.1117/12.2564630

13. Saleh S.M., Almotiri M.K., Ali R. Green synthesis of highly luminescent gold nanoclusters and their application in sensing Cu (II) and Hg (II) // Journal of Photochemistry and Photobiology A: Chemistry. 2022. Vol. 426. P. e113719. doi: 10.1016/j.jphotochem.2021.113719

14. Holt D., Okusanya O., Judy R., et al. Intraoperative near-infrared imaging can distinguish cancer from normal tissue but not inflammation // PLoS One. 2014. Vol. 9, N 7. P. e103342. doi: 10.1371/journal.pone.0103342

15. Newton A.D., Kennedy G.T., Predina J.D. Intraoperative molecular imaging to identify lung adenocarcinomas // Journal of Thoracic Disease. 2016. Vol. 8, N 9S. P. S697–S704. doi: 10.21037/jtd.2016.09.50

16. Рында А.Ю., Олюшин В.Е., Ростовцев Д.М., Забродская Ю.М., Папаян Г.В. Сравнительный анализ флуоресцентной навигации в хирургии злокачественных глиом с использованием 5-АЛА и хлорина Е6 // Хирургия. Журнал им. Н.И. Пирогова. 2022. № 1. С. 5–14. doi: 10.17116/hirurgia20220115

17. Li C.H., Kuo T.R., Su H.J., et al. Fluorescence-guided probes of aptamer-targeted gold nanoparticles with computed tomography imaging accesses for in vivo tumor resection // Scientific Reports. 2015. Vol. 5. P. e15675. doi: 10.1038/srep15675

AUTHORS' INFO

*** Tatiana N. Zamay,** Dr. Sci. (Biology);
address: 1 Partizan Zheleznyak street, Krasnoyarsk 660022, Russia;
ORCID: 0000-0002-7493-8742;
eLibrary SPIN: 8799-8497;
e-mail: tzamay@yandex.ru

Galina S. Zamay, Cand. Sci. (Biology);
ORCID: 0000-0002-2567-6918;
eLibrary SPIN: 6501-0371;
e-mail: galina.zamay@gmail.com

Daniil S. Chumakov, Cand. Sci. (Biology);
ORCID: 0000-0003-1658-2562;
eLibrary SPIN: 8491-2313;
e-mail: laik2012@yandex.ru

Semen A. Sidorov;
ORCID: 0000-0001-6676-6656;
eLibrary SPIN: 8740-5259;
e-mail: sidorov.syoma2014@yandex.ru

Aleksey V. Krat, MD, Cand. Sci. (Medicine);
ORCID: 0009-0006-5357-2637;
eLibrary SPIN: 2846-8592;
e-mail: alexkrat@mail.ru

Boris N. Khlebtsov, Dr. Sci. (Physics and Mathematics);
ORCID: 0000-0003-3996-5750;
eLibrary SPIN: 5274-8718;
e-mail: khlebtsov_b@ibppm.ru

ОБ АВТОРАХ

*** Замай Татьяна Николаевна,** д-р биол. наук;
адрес: Россия, 660022, Красноярск, ул. Партизана Железняка, д. 1;
ORCID: 0000-0002-7493-8742;
eLibrary SPIN: 8799-8497;
e-mail: tzamay@yandex.ru

Замай Галина Сергеевна, канд. биол. наук;
ORCID: 0000-0002-2567-6918;
eLibrary SPIN: 6501-0371;
e-mail: galina.zamay@gmail.com

Чумаков Даниил Сергеевич, канд. биол. наук;
ORCID: 0000-0003-1658-2562;
eLibrary SPIN: 8491-2313;
e-mail: laik2012@yandex.ru

Сидоров Семён Александрович;
ORCID: 0000-0001-6676-6656;
eLibrary SPIN: 8740-5259;
e-mail: sidorov.syoma2014@yandex.ru

Крат Алексей Васильевич, канд. мед. наук;
ORCID: 0009-0006-5357-2637;
eLibrary SPIN: 2846-8592;
e-mail: alexkrat@mail.ru

Хлебцов Борис Николаевич, д-р физ.-мат. наук;
ORCID: 0000-0003-3996-5750;
eLibrary SPIN: 5274-8718;
e-mail: khlebtsov_b@ibppm.ru

Irina A. Shchugoreva, Cand. Sci. (Chemistry);
ORCID: 0000-0003-4207-1627;
eLibrary SPIN: 8826-6672;
e-mail: shchugorevai@mail.ru

Anastasia A. Koshmanova;
ORCID: 0000-0001-7339-8660;
eLibrary SPIN: 2217-2229;
e-mail: koshmanova.1998@mail.ru

Ruslan A. Zukov, MD, Dr. Sci. (Medicine);
ORCID: 0000-0002-7210-3020;
eLibrary SPIN: 3632-8415;
e-mail: zukov.ra@krasgmu.ru

Nikolai G. Khlebtsov, Dr. Sci. (Physics and Mathematics);
ORCID: 0000-0002-2055-7784;
eLibrary SPIN: 4377-1257;
e-mail: khlebtsov@ibppm.ru

Anna S. Kichkailo, Dr. Sci. (Biology);
ORCID: 0000-0003-1054-4629;
eLibrary SPIN: 5387-9071;
e-mail: annazamy@yandex.ru

Щугорева Ирина Андреевна, канд. хим. наук;
ORCID: 0000-0003-4207-1627;
eLibrary SPIN: 8826-6672;
e-mail: shchugorevai@mail.ru

Кошманова Анастасия Андреевна;
ORCID: 0000-0001-7339-8660;
eLibrary SPIN: 2217-2229;
e-mail: koshmanova.1998@mail.ru

Зуков Руслан Александрович, д-р мед. наук;
ORCID: 0000-0002-7210-3020;
eLibrary SPIN: 3632-8415;
e-mail: zukov.ra@krasgmu.ru

Хлебцов Николай Григорьевич, д-р физ.-мат. наук;
ORCID: 0000-0002-2055-7784;
eLibrary SPIN: 4377-1257;
e-mail: khlebtsov@ibppm.ru

Кичкайло Анна Сергеевна, д-р биол. наук;
ORCID: 0000-0003-1054-4629;
eLibrary SPIN: 5387-9071;
e-mail: annazamy@yandex.ru

* Corresponding author / Автор, ответственный за переписку